Supporting Information

Janus Polymeric Discs by Seeded Swelling Emulsion Polymerization

Linlin Zhang,[*a,b] *Fuyan Huang,* [a] *Shiyu Du,* [a] *Guolin Zhang* [c] *and Dayin Sun*[*b]

[a]Liaoning Provincial Key Laboratory for Synthesis and Preparation of Special Functional Materials, Shenyang University of Chemical Technology, Shenyang 110142, China.

[b]Institute of Polymer Science and Engineering, Department of Chemical Engineering, Tsinghua University, Beijing 100084, China.

[c]Liaoning Provincial Key Laboratory for Green Synthesis and Preparative Chemistry of Advanced Materials, Liaoning University, Shenyang 110036, China.

*E-mail: zhanglinlin@syuct.edu.cn

*E-mail: sundayin@tsinghua.edu.cn

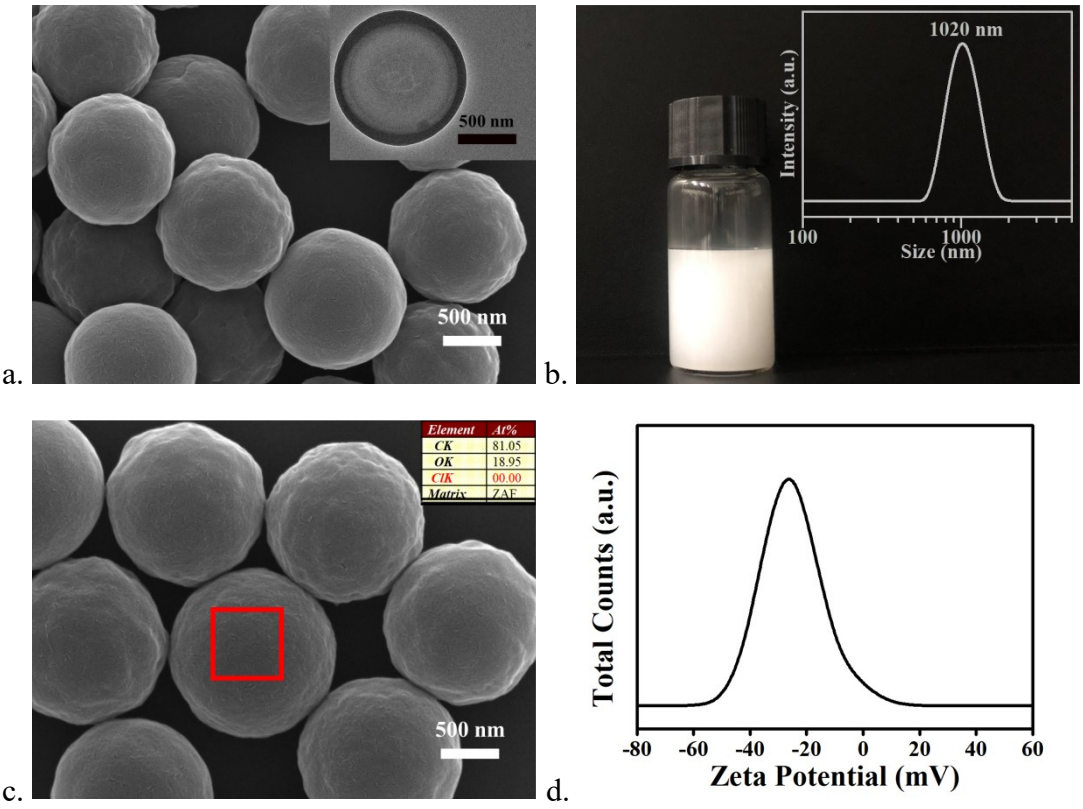

Figure S1. (a) SEM and inset TEM images of the PS hollow sphere seed (HP-1055); (b) the aqueous dispersion and the inset DLS trace; (c) EDX spectrum of the PS hollow sphere, no Cl element present at the sphere; (d) Zeta potential of the PS hollow sphere seed aqueous dispersion.

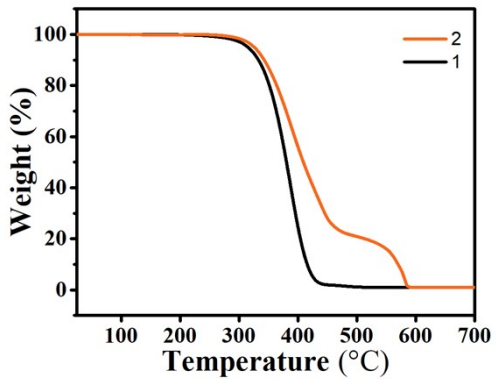

Figure S2. TGA traces of (1) the PS hollow sphere (HP-1055) and (2) the PS@*c*PVBC composite sphere.

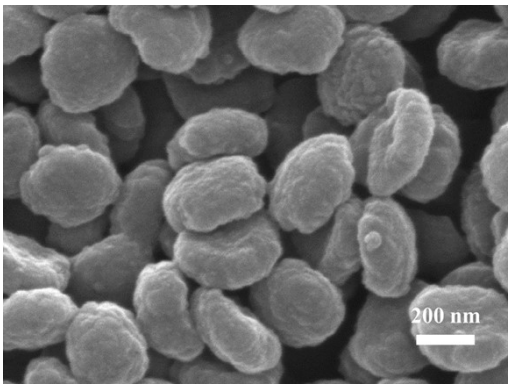

Figure S3. SEM image of the *c*PVBC disc after the polymerization for 12 h.

a. 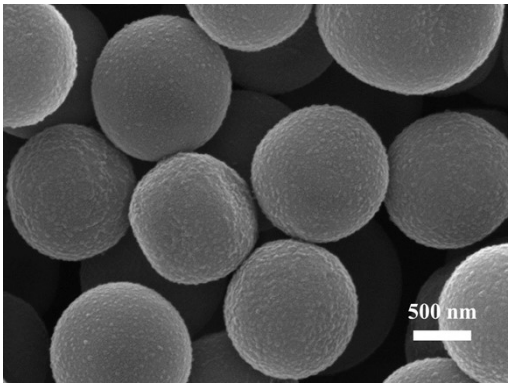

b. 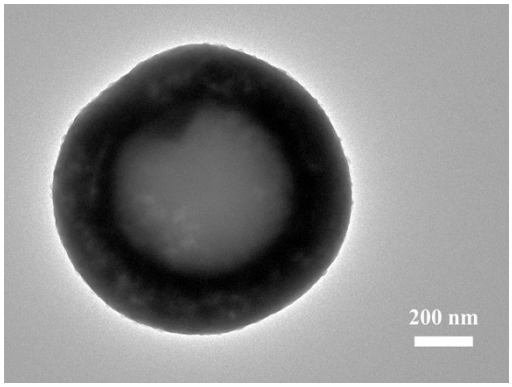

Figure S4. (a) SEM and (b) TEM images of the PS/*c*PVBC composite sphere after the polymerization at DVB/VBC ratio of 4/1. The sphere was treated with DMF.

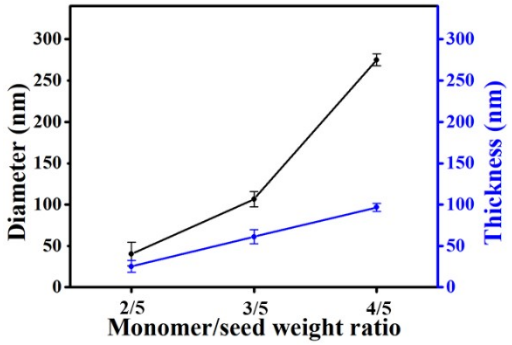

Figure S5. Dependences of diameter and thickness of the *c*PVBC discs on monomer/seed ratio.

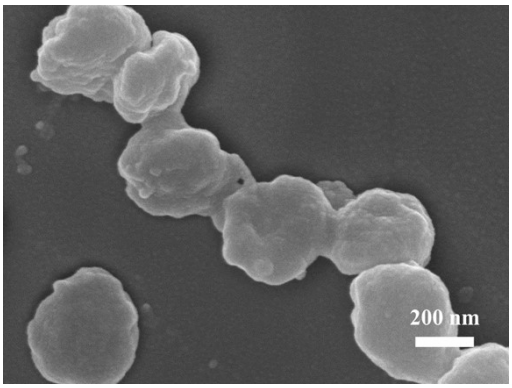

Figure S6. SEM image of the *c*PVBC disc synthesized at the monomer/seed ratio of 5/5.

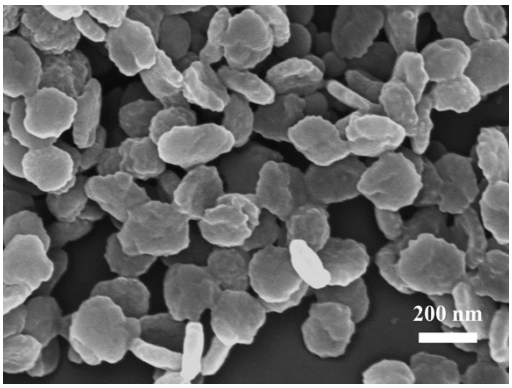

Figure S7. SEM image of the *c*PVBC disc by the polymerization at 1.5 wt% of AIBN.

a.

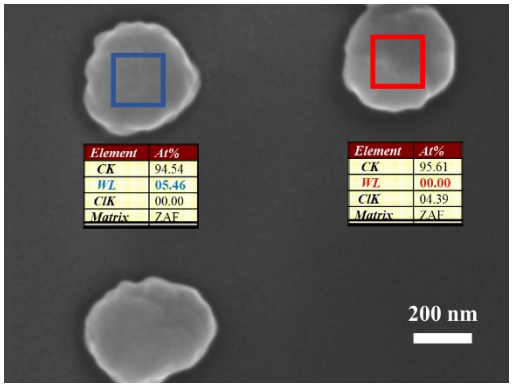

b.

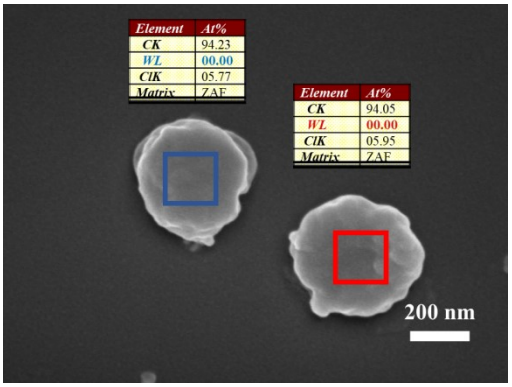

Figure S8. EDX results of (a) the Janus disc of *c*PVBC-PEO and (b) the disc of *c*PVBC. The two samples were treated by labelling with phosphotungstic acid (PTA).

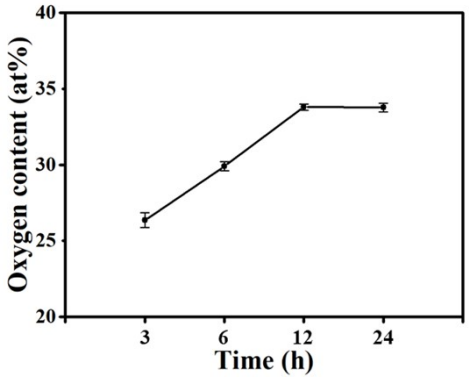

Figure S9. Oxygen content at convex side of the Janus disc of *c*PVBC-PEO with increasing the nucleophilic substitution time.

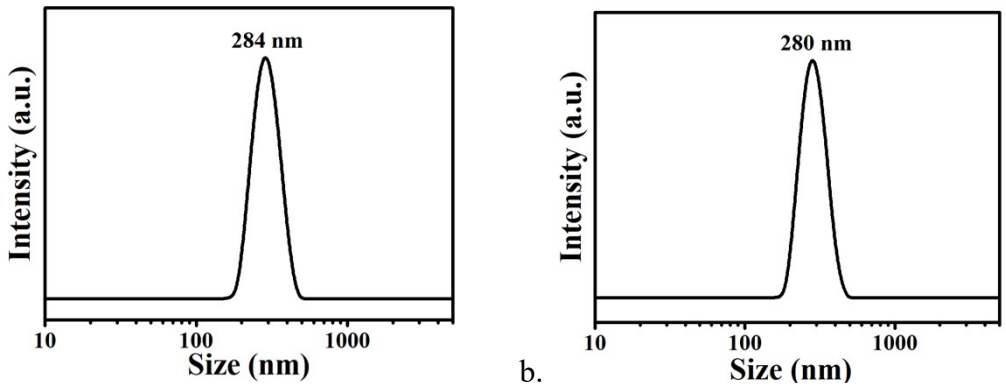

Figure S10. DLS traces of (a) the Janus disc of PNIPAM-*c*PVBC-PEO and (b) the Janus disc of *c*PVBC-PEO. The two samples were dispersed in ethanol.

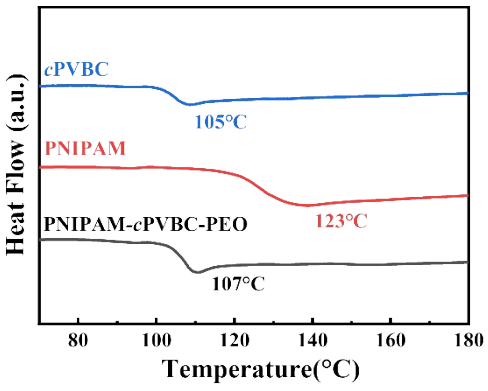

Figure S11. DSC curves of *c*PVBC, PNIPAM and PNIPAM-*c*PVBC-PEO Janus discs, with their glass transition temperatures marked.

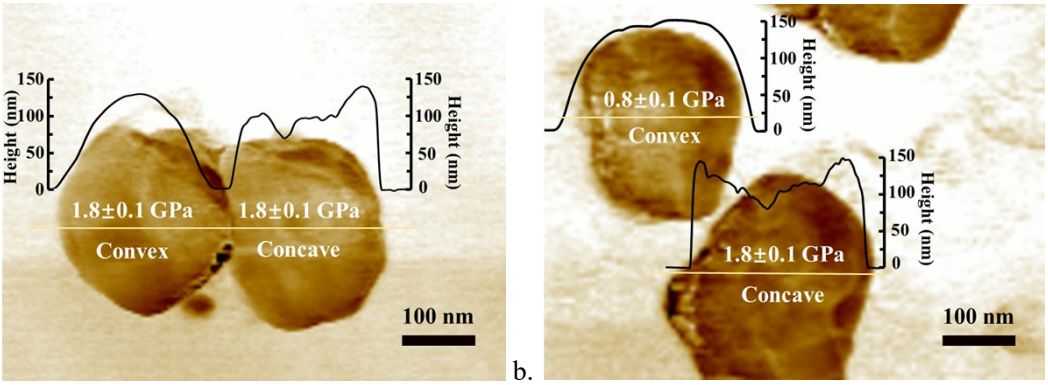

Figure S12. Distinguishing convex and concave sides of the discs by AMF height imaging: (a) *c*PVBC; (b) *c*PVBC-PEO. Moduli were measured at the convex and concave sides.

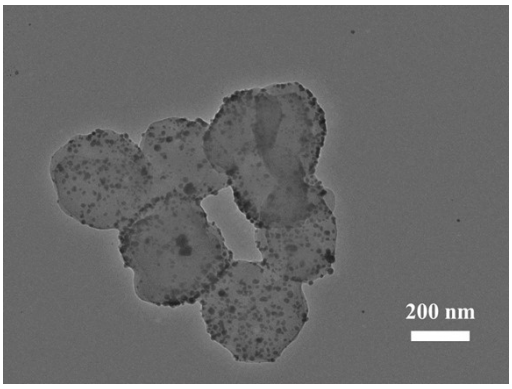

Figure S13. TEM image of the disc of PNIPAM-*c*PVBC-PEO after labelling with Au NPs.

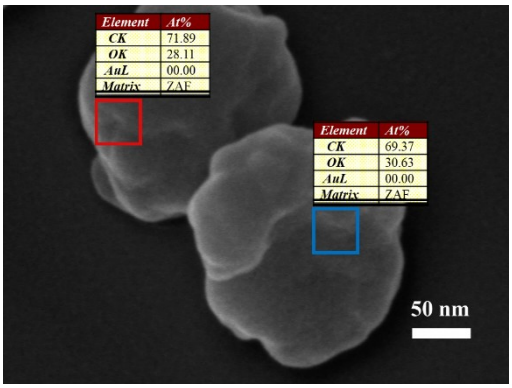

Figure S14. SEM image and EDX result of the *c*PVBC-PEO disc after treatment with Au NPs.

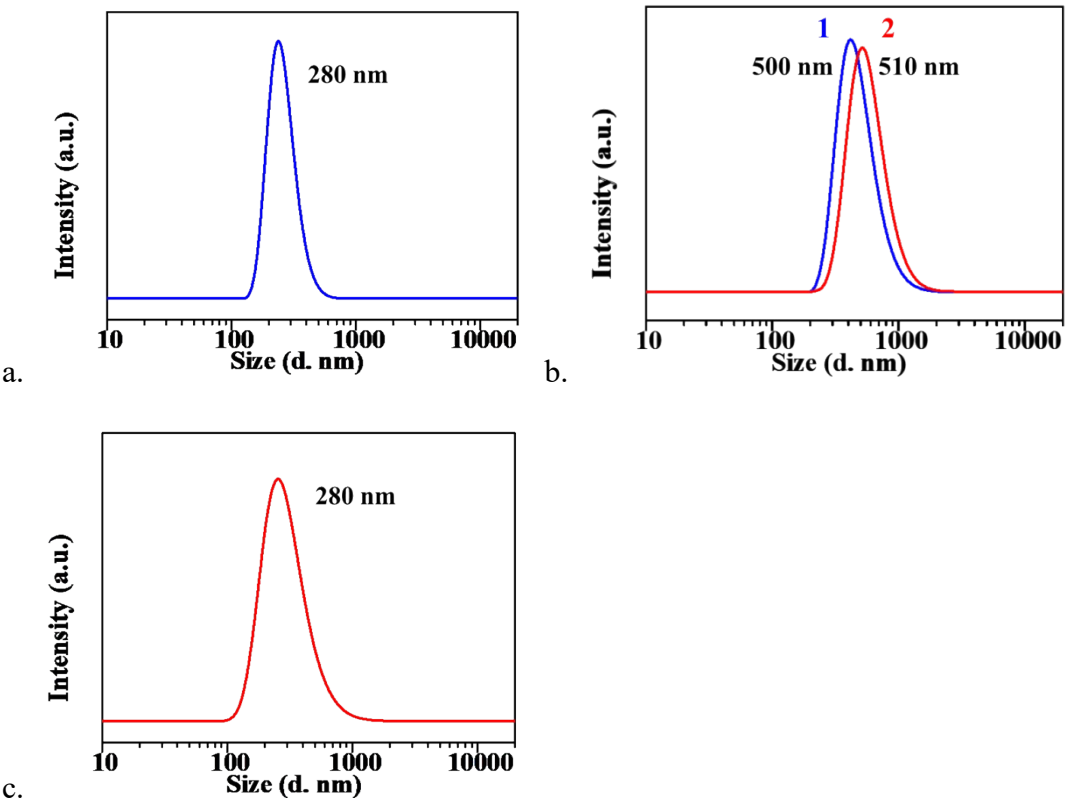

Figure S15. (a) DLS trace of PNIPAM-*c*PVBC-PEO in water at 25 ℃; (b) (1) in water and (2) *n*-decane at 40 ℃; (c) DLS trace of PNIPAM-*c*PVBC-PEO in *n*-decane at 85 ℃.

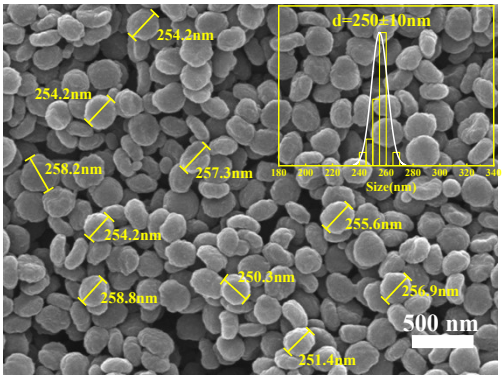

Figure S16. SEM image of PNIPAM-*c*PVBC-PEO disks (inset: particle size distribution).